Study of the Effect of the Mineral Feed Size Distribution on a Ball Mill Using Mathematical Modeling

Rodríguez-Torres, Israel; Perez-Alonso, Cristobal; Delgadillo, Jose Angle

Instituto de Metalurgia–Facultad de Ingeniería, Universidad Autónoma de San Luis Potosí, 78210 San Luis Potosí, SLP, MÉXICO

Espinosa, Erik; Rosales-Marín, Gilberto*+

Ingeniería de Minerales–Coordinación Académica Región Altiplano, Universidad Autónoma de San Luis Potosí, 78700 Matehuala, SLP, MÉXICO

ABSTRACT: *In this paper, the effect of the feed size distribution was studied for a ball mill. Copper ore of 0.5% was tested using batch-grinding tests. Samples were carried out using three reconstructed feed size distributions in an experimental ball mill. The size distribution was reconstructed using the double Weibull formula, and modeled using the selection and breakage functions. Copper ore samples were grinding up to 15 min. A nanosize (–19+12.5), coarse (–19+6.3 mm), medium (–4.75+0.6 mm), and fine (+0.425–0.038 mm) particle size distributions were tested. The 0.32 m diameter test mill was run at 38% volume loading and Nc (critical speed) of 68% (50.85 rpm). Breakage rate parameters were calculated and simulated for each size distribution in an industrial mill. The results show that the change in the feed size distribution has an impact on the grinding kinetics. The curves show that the mono size fraction has the highest specific rate of breakage. It is also important to note that, as the size distribution F80 decreases the power consumption increases.*

KEYWORDS: *Ball mill; Comminution; Mathematical modeling; Mineral feed size distribution; PBM modeling.*

INTRODUCTION

Grinding is an energy-intensive operation in which energy losses occur in heat and noise. This energy is not utilized in the grinding process. The quantification of the applied specific impact energy and particles' internal fracture energy (utilized) have been studied in fundamental research [1-3]. Since the size reduction in tumbling mills is not an energy-efficient operation and quite a few studies have been carried out to make grinding more efficient so far.

In mineral processing, tumbling mills have been used for more than a century. Nowadays, the modeling for scale-up of a ball mill uses wet grinding purposes. This is a relatively new and novel approach due is more significant and common than dry grinding [4]. However, there is still a need for understanding complete mechanisms in grinding to make it more efficient. *Herbst et al.* [5] developed kinetic approaches of breakage in the mills.

** To whom correspondence should be addressed.*
+ E-mail: gilberto.rosales@uaslp.mx
1021-9986/2021/1/303-312 10/$/6.00

One example of these approaches is the Population Balance Model (PBM) [6-8] that uses the selection function, S_i, (rate of breakage) and breakage distribution function. When the rate of breakage is normalized by energy (E), it is called a specific selection function, S_i^E [7].

THEORETICAL SECTION

The selection and breakage functions are the main components of the batch population balance (PBM) equation. Breakage function is determined by a series of grinding tests, whereas the selection function is usually back-calculated or directly estimated from energy studies. The breakage rate is the key parameter for PBM approach. So far, several different approaches for the estimation of selection functions have been proposed. Such as those based on the probability of capture and nipping [9], based on impact energy spectra [1-3, 10], and based on the probability of breakages [11-13]. However, in this study, the main calculations were made based on *Austin* and *Herbst-Fuerstenau's* [7] selection function approaches. In the analysis of the materials breakage, it may be useful to make an initial assumption that the breakage of each size fraction is the first order in nature [14]. The selection function can be defined as the rate that the particle breaks into smaller sizes. The breakage function is the distribution of particles after the breakage occurs.

The fundamental logic behind the PBM may be explained specifically formulated as a numeric balance. The size discretized batch PBM is expressed as follows:

$$\frac{dw_i}{dt} = -S_i w_i(t) + \sum_{\substack{j=1 \\ i>1}}^{i-1} b_{ij} S_j w_j(t), \quad n \geq i \geq j \geq 1 \tag{1}$$

Where b_{ij} is the fraction of broken mass of size class j appearing in size class i, and S_i is the fractional rate of breakage of size class i. Equation 1 was analytically solved [15]. The system of solution for the size classes can be written as follows:

$$w_i(t) = \sum_{j=1}^{i} d_{ij} w_j(0) \quad , \quad i \geq 1 \tag{2}$$

where $d_{ij}(t)$ is represented by:

$$d_{ij}(t) = \begin{cases} 0 & i < j \\ e^{-S_i t} & i = j \\ \sum_{k=j}^{i-1} C_{ik} C_{jk} \left(e^{-S_k t} - e^{-S_i t} \right) & i > j \end{cases} \tag{3}$$

and c_{ij} is:

$$G_{ij}(t) = \begin{cases} & i < j \\ \sum_{k=i}^{j-1} C_{ik} C_{jk} & \\ 1 & i = j \\ \left(\frac{1}{S_i - S_j} \right) \sum_{k=j}^{i-1} S_k b_{ik} C_{jk} & i > j \end{cases} \tag{4}$$

Several authors [5, 7, 16] have applied the selection function for scaling up through the specific selection function. The specific selection function is proportional to the mass-specific power input to the mill:

$$S_i^E = S_i \frac{M}{P} \tag{9}$$

Where M is the mass of the charge in the mill excluding the media and P is the basic mill power drawn equation [17] is given by:

$$P = \frac{2\pi N \tau}{60} \tag{10}$$

Where N is the mill speed in rpm, τ is the torque exerted by the mill minus friction on the bearings. The breakage function (b_{ij}) could be calculated using Equation (5), using the next equation [15]:

$$B_{ij} = \varnothing \left(\frac{x_{i-1}}{x_j} \right)^{\alpha_2} + (1 - \varnothing) \left(\frac{x_{i-1}}{x_j} \right)^{\alpha_3} \tag{11}$$

The $B_{i,j}$ function describes the size distribution of the fine fraction in the population of progeny particles. x_i is the top value of the size interval is indexed by i. Parameters $\varnothing, \alpha_2$ and α_3 are the model parameters to be adjusted from the experimental data. B_i is the cumulative form of the b_{ij} function, as shown in equation 12.

$$b_{ij} = \begin{cases} B_{i,j} - B_{i+1,j} & i > j \\ 1 - \sum_{i}^{n-1} b_{i,j} & i = n \\ 0 & i \leq j \end{cases} \tag{12}$$

Table 1: Experimental feed distribution criterion.

Test	Type	Screen Size (mm)
1	Coarse feed SD	19, 12.5, 9.5, 6.3
2	Medium feed SD	4.75, 3.35, 2.36, 1.7, 1.4, 0.85,0.6
3	Fine feed SD	0.425, 0.3, 0.212, 0.15, 0.106, 0.075, 0.053, 0.045, 0.038

Table 2: Weibull double parameters formula.

Parameters	Coarse SD	Medium SD	Fine SD
β	0	0	0
F_{80}(μm)	13802.274	3273.46	379.325
γ	0.622	0.985	0.831
ø	3.950	0.5406	1.321

$B_{i,j}$ represents the cumulative weight fraction of material broken from size *j* which appears in size interval *i*. The subscript 1 refers to the original material of size 1 at time t = 0, the subscript *i* refers to a smaller size than the size *j* and the subscript *j* refer to the size from which material that appears in size *i* is broken.

$$\varnothing = \alpha_1 \cdot \left[\frac{X_i}{X_1}\right]^{-\delta} \quad (13)$$

where δ characterizes the degree of non-normalization.

EXPERIMENTAL SECTION

A 0.5% Cu ore sample ($CuFeS_2$) was used in this study. A mono size fraction (–19 mm + 12.5 mm) and three full-Size Distributions (SD) were prepared for each sample identified as Coarse, Medium, and Fine distribution. Screen analysis was performed using $\sqrt{2}$ screen series starting from 19 mm down to 0.038 mm as shown in Table 1.

The amount of dry mass used in each fraction was calculated using a variation of a Rosin Rammler double Weibull distribution as shown in Equation (15).

$$Y_i = \left\{\beta\left[1 - e^{\ln 0.2 * \left(\frac{F}{F_{80}}\right)^{\gamma}}\right] + (1-\beta)\left[1 - e^{\ln 0.2 * \left(\frac{F}{F_{80}}\right)^{\varnothing_1}}\right]\right\} \times 100 \quad (15)$$

Where Y_i is the percent passing in a natural distribution, β refers a logical argument which denotes the type of distribution to be used; (if this argument is TRUE Weibull Cumulative Distribution Function is used if it is FALSE Weibull Probability Density Function is used), F_{80} means the 80% passing in the feed (μm), F is the mesh opening (μm), γ refers to the shape factor for the finest and $\emptyset_1$the shape factor for the coarse. The coarse distribution has a F_{80} value of 13.808 mm, the medium and fine distribution has 4.826 mm and 0.379 mm respectively. The F_{80} proposed was selected according to a similar full-size distribution of a tertiary crushing stream divided in three sections. Table 2 shows the parameter calculated values used to match the feed size distributions.

The re-constructed feed size distributions were used as a reference to determine the experimental feed size distribution. The amount of ore (g) in each mesh was calculated to obtaining the size distribution which is presented in Fig. 1.

Grinding tests

The feed distributions in Fig. 1 were used to perform the grinding tests. Four grinding time intervals (0.5, 1, 2, and 15 min.) were used for each size distribution. The feed distribution was kept constant in each test and then loaded in the mill for batch grinding. After the grinding time, the mill content was discharged, and the particle size analysis was done on the product using screens at an interval of $\sqrt{2}$ and the material contained in each screen was weighed. The top screen size for the product was 19,500 μm and the down screen size was 38 μm. After this, the material was recovered and used for the next grinding time.

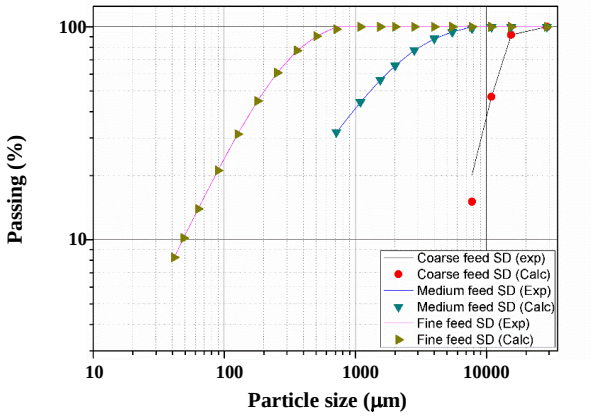

Fig. 1: Experimental and calculated feed size distributions.

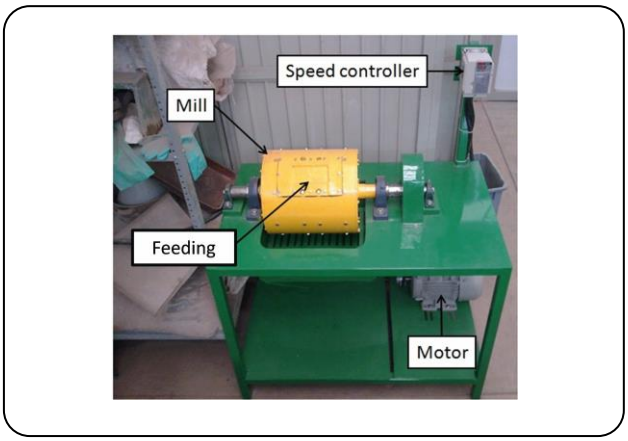

Fig. 2: Experimental setup.

The ore density was 3.18 g/cm^3 and the feed distribution re-constructed was used. The laboratory mill used for the batch grinding test for the chalcopyrite sample has an inside diameter of 0.32 m and a length of 0.35 m (Fig. 2).

The charge level was set at 38% for all tests at 68 solids percent. The mill motor has a digital control unit that was used to set the mill speed around 50.83 rpm (68% of Nc). The optimal ball size was obtained using equation 16 [18-19]:

$$B_S = 1.354\,(F_{80})^{0.5}\left[\frac{\rho_{ore}\,W_{iB}}{N_c\,D^{0.5}}\right]^{\frac{1}{3}} \qquad (16)$$

B_S is the optimal Ball size, F_{80} represents 80% passing size in the fresh feed stream, D is the inner diameter, ρ_{ore} is the ore specific gravity. W_{iB} was calculated in eight cycles based on Bond´s experimental procedure [18-19].

The size distribution of balls inside the mill follows Gates-Gaudin-Schumann):

$$G(x) = 100\left[\frac{g}{k_{100}}\right]^{m} \qquad (17)$$

Where $G(x)$ is percent retained in "x" mesh, k_{100} represents the 100% passing size in the lineal function and m is the slope in the line equation. The size distribution of balls is showed in Table 3.

RESULTS AND DISCUSSION

Fig. 3 shows the percent cumulative from –38+20 µm the plots obtained in this fraction for all sizes distributions. It is clearly seen that the breakage process follows first-order kinetics. The determination of R^2 has values between 0.9992 from Mono size fraction to 0.9997 from Fine feed SD. As discussed before, the feed is not the mono size in all the samples studied in this paper but the first order law is in good agreement for smaller sizes used (–1180+850 to –38+20 µm). However, for large sizes in Mono size fraction, Coarse SD and Medium SD (–12500+9500 to –2360+1700 µm) and Fine SD (–600+425) the first-order law does not apply satisfactorily.

An example of the deviation from first-order kinetics is presented in Fig. 4. Fig. 4 shows the fraction of -12500+9500 µm for the samples of Mono size fraction, Coarse SD and Medium SD. The same variation is present in the coarse part of Fine SD at the fractions –600+425 mesh. This deviation can be explained by the fact that the coarse particles are difficult to be ground by the mill then the grinding rate decreases. The energy applied in the mill is just enough to take some coarse particles to the fracture point. This mechanism is known as cleavage [20]. Around this point, the breakage rate decreases with time in a non-linear manner [21] and the progeny size is comparatively close to the original size. The fine particles may then cause the slowing down in the breakage, due to the low capacity of the lifters to move it around the mill. This causes agglomeration of fine particles in the mill base and bed particle appears. This limits the probability of ball-ore-ball impact and the ore fracture due to contracting. The impact is absorbed like a hydraulic shock absorber [22].

Rate of breakage

The model parameters, α, μ and Λ were calculated combining Equation 7 and 8 by a non-linear regression

Table 3: Gates-Gaudin-Schumann model parameters and ball size distribution.

Experimental characteristics				Ball size (mm) m= 4.8	Percent Distribution k_{100}= 76.2
W_i (kWh/t)	10.12	Ore	$CuFeS_2$		
Motor Power (Hp)	3	ρ_{ore} (ton/m^3)	3.18	76.2	48.7
D (m)	0.32	F_{80} (µ)	9´500	63.5	49.6
Length (m)	0.35	Critical Speed (%)	55	50.8	1.65
Level Charge (%)	35	Grinding Times (min)	0.5, 1, 2 and 15		

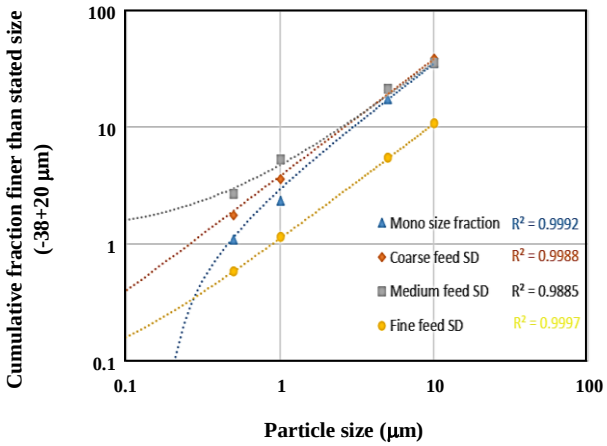

Fig. 3: Cumulative fraction finer than stated size vs grinding time.

technique. The general equation that shows the specific rate of breakage is expressed as:

$$S_i^E(d) = \frac{a \cdot \left\lceil \frac{X_i}{X_0} \right\rceil^{\alpha}}{1 + \left\lceil \frac{X_i}{\mu} \right\rceil^{\Lambda}} \cdot \frac{M}{P} \qquad (18)$$

Where the parameter a represents the intersection of the axis in a plot (selection function versus particle size), α is the slope of the line, μ is the critical point where line change direction and decrease. M is the total grinding mass used, P is the power drawn used for determinate the specific energy (kWh/ton). The rate of breakage (S_i) and the specific breakage rate (S_i^E) values vary with the size. The specific rate of breakage increases up to a maximum feed size and decreases rapidly above this size fraction. This means that there is an optimal feed size for the mill. These values are described by the parameter μ and it is where the maximum breaks occur. After of μ values of the breaks increase slowly. The parameter Λ was kept constant according to Austin's value [23]. α, which is characteristic of the material, was satisfactorily determined and kept constant for the cases of mono size fraction, Coarse, Medium, and fine particle size distributions.

The specific rate of breakage parameters was estimated by using the non-linear regression technique, fitting the S_i in Equation 18. Basically, this technique finds the best combination of fitting parameters of a model by minimizing the square of the differences between the experimental values $P_{exp}(t)$ and the predicted ones $P_{model}(t)$ [24]. The parameters of the specific rate of breakage can be seen in Fig. 5. The calculated parameters for the studied samples are shown in Fig. 6.

The value for parameter Λ was chosen from the literature to start the calculation [14]. α, which is characteristic of the material, was properly determined and kept constant. The parameter α is a positive number normally in the range of 0.5 – 1.5. It is characteristic of the material and does not vary with mill operating conditions (rotational speed, ball load, ball size, or mill hold-up) over the studied test ranges [6] for dry milling. The a and μ parameters which vary with the mill conditions were determined using the same technique. The parameter μ is the critical point where the line changes direction and decrease. This parameter μ is related to x_m since both are dependent on where the curve-specific rate of breakage vs. particle size starts to bend. The values of μ were found to be directly proportional to the corresponding values of x_m for each grinding media. The parameter a is directly proportional to the specific rate of breakage. It is expressed in time^{-1}. The parameters calculation for each size distribution can be observed in Table 4.

For this study the $B_{i,j}$ values are assumed to be normalizable ($\delta = 0$). This means that the fraction appearing at a size less than the initial feed size and is

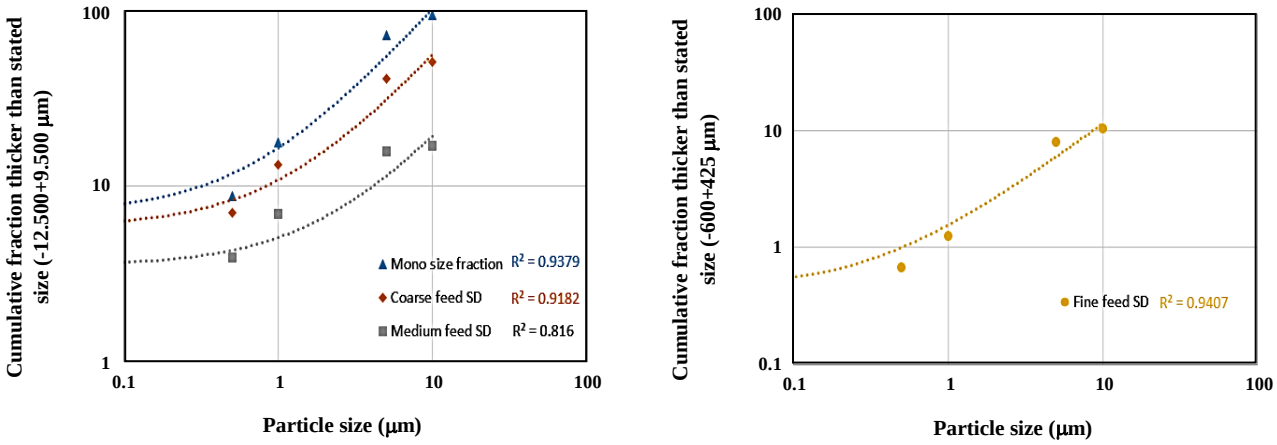

Fig. 4: Cumulative fraction thicker than stated size vs grinding time.

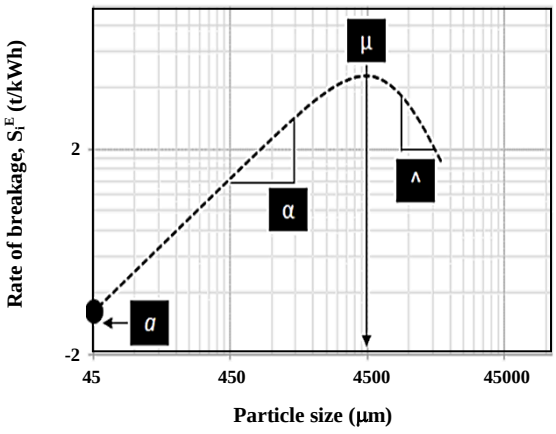

Fig. 5: Graph showing the parameters obtained in S_i^E versus particle size.

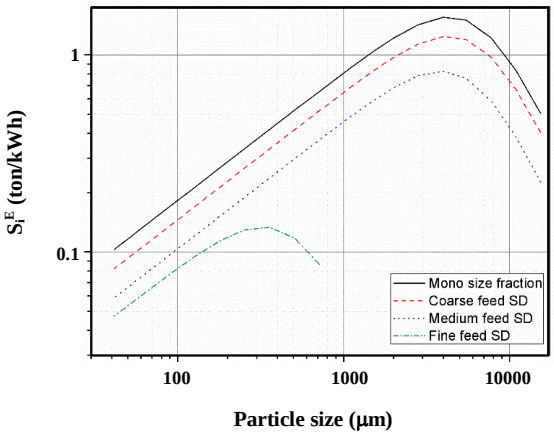

Fig. 6: A graph showing S_i^E versus particle size.

independent of the initial feed size. The functional form of the $B_{i,j}$ is given in Equation 12. α_1 is the amount of progeny that contributes to the production of the finer fraction. The different values of, α_2 and α_3 describe the larger products produced by tensile stress and the smaller products produced by the intense compressive stress at the points of application. The parameter values for $B_{i,j}$ were determined from Equation 21 using the BII method [14]. The α_1, α_2, and α_3 are the model parameters. These parameters were determined by a non-linear regression technique assuming constant values of S_i in the population balance model.

In a ball mill, there are many zones where the size reduction occurs usually know as load profile. The load profile in a ball mill basically is governed by two fracture mechanisms that predominate: impact and abrasion. The ball mill zones are shown in Fig. 7.

The mono size fraction has a higher rate of breakage 0.00918 min^{-1}, this can be explained by the fact that the mill lifters can easily lift the load up to a higher point (load shoulder) from which it subsequently precipitates up to load kidney. In the Mono size fraction sample, its principal mechanism size reduction is the impact, which produces the most fraction of daughter products that contribute to the finer fraction, this could be validated for the α_1 value is slightly higher than the others.

The fine feed size distribution has the lowest rate of breakage 0.00421 min^{-1}, this may occur due to these size distributions have a lot of fine particles. These particles take a place into the load kidney were the principal

Table 4: S_i^E and B_{ij} calculated parameters.

Parameters	Specific Selection Function					Breakage function		
	S_1^E	a	α	Λ	μ	α_1	α_2	α_3
Units	(t/kWh)	min^{-1}	----	----	µm	----	----	----
MS (-19+12.5 mm)	0.5069	0.00918	0.650	2.5	6532.351	0.2436	0.250	4.0
Coarse feed SD	0.4043	0.00732	0.650	2.5	6531.230	0.3145	0.250	4.0
Medium feed SD	0.2265	0.00521	0.650	2.5	5876.283	0.3243	0.250	4.0
Fine feed SD	0.0111	0.00421	0.650	2.5	686.23	0.2945	0.251	4.1

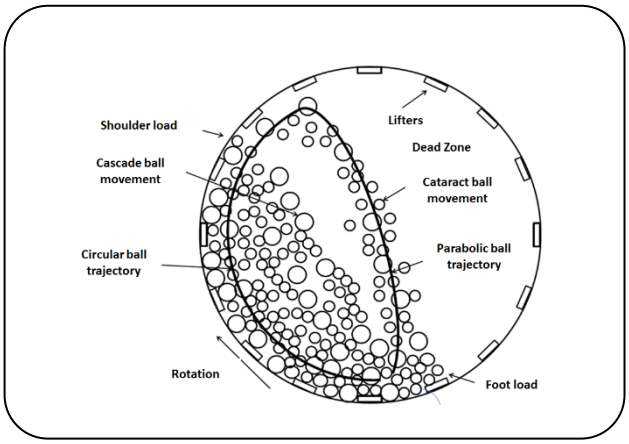

Fig. 7: Zones in a ball mill reduction.

the mechanism is the abrasion. The abrasion mechanism produces slowly more fine particles may then causing the slowing down in the breakage, due to the low capacity of the lifters to move it around the mill. This causes agglomeration of fine particles in the mill base and a bed particle appears. This limits the probability of ball-ore-ball impact and the ore fracture due to contracting. The impact is absorbed like a hydraulic shock absorber [22]. For this sample the α_1 value has the lower values of all samples, this means that the fine fraction contribution in the grinding kinetic is not as effective as the previous samples.

In all cases when there was a change of size distribution the values of α_2 and α_3 was small variations, which means, that the larger products produced by tensile stress and the smaller products produced by the intense compressive stress are a little higher in each size distribution. Due α_3 is the input of breakage for cleavage, can express that this breakage mechanism varies in all cases.

Energy consumption

Table 5 shows the energy consumption for all the samples studied in this paper. Measurement of the energy consumption was made by a programmable analog variator. The variator used in a grinding kinetic measures voltage and amperage every millisecond and could be extracted in a report. Four reports of voltage and amperage were generated per sample and according to the grinding time. Finally, the kWh in each sample was calculated. The specific energy (kWh/ton) depends on the operating conditions and the mill geometry and it has been calculated for each feed size distribution.

Fig. 8 shows the graph where the Mono size fraction is the best of all experiments, due to this sample, has lower power consumption but a higher rate of breakage. The experiment that has the lowest fracture ranges and a high-energy consumption is the Fine feed SD. It is interesting to note that even fine particles are added, the range of fracture decreases, and the energy consumption increases.

Mill Product

The experimental and simulated cumulative passing data were compared for validation purposes by using the parameters are given in Table 4. Fig. 9 shows the predicted and the experimental data for a mono size fraction, coarse, medium, and fine feed sizes distributions. For the cases of mono size, coarse, and medium feed sizes distributions, the prediction of the model shows good data reproduction. A little variation between experimental and modeling values shows that the model can efficiently reproduce the data modeling for all cases. For the case of fine feed size distribution, a little variation between experimental and prediction is denoted. This may occur for the fact that the fine particles into a ball mill follow non-first-order breakage kinetics as described before. [19]). Generally, in any event of size reduction, a small particle size usually requires more energy for a fracture event to occur, but

Table 5: Energy consumption in a ball mill grinding kinetics.

Type	Energy consumption	
	kWh	kWh/ton
Mono size fraction	0.4749	9.5361
Coarse feed SD	0.4750	9.5382
Medium feed SD	0.4760	9.5582
Fine feed SD	0.4861	9.7610

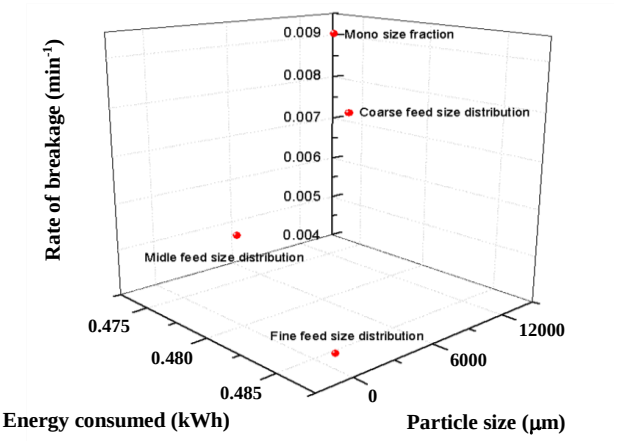

Fig. 8: Comparison chart between particle size, the rate of breakage, and the specific energy used.

when the breakage occurs, the abrasion between particles generates a progeny of finer particles. This progeny in most cases needs a lot of time to produce it.

CONCLUSIONS

In this paper, an experimental method together with modeling is used to investigate the effect of the feed size distribution on the grinding process. Four different types of feed were designed using the Weibull distribution. The mill's inside conditions (design and operating) other than feed size distribution were kept constant. The same type of lifters, critical speed, loading amount of ball, and material aimed to investigate feed size distribution effect only. A kinetic approach was used to calculate rate parameters. The breakage function was evaluated for fine and coarser particles and was assumed to be normalizable and the breakage rate parameters were determined. Following conclusions are drawn from the study:

The selection function was evaluated for coarser, medium, and fine size distribution while the breakage function is assumed to be normalizable.

The breakage rate parameters were satisfactorily determined. The S_i^E curves show that the mono size fraction distribution shows the highest rate of breakage: S_1^E values of 0.00918 min^{-1}. Fine feed size distribution being the least efficient: S_1^E 0.00421 min^{-1}.

In general, the change in the feed size distribution has an impact on the grinding kinetics. If it is considering that the mono size fraction as a starting point, adding fine particles causes a change in the F_{80}, this causes changes in the charge profile affecting the energy consumption.

In the samples studied in this paper with size distributions (Coarse feed SD, Medium feed SD, and Fine feed SD), it can be concluded that the highest rate of breakage is the size distribution which contains a large number of coarse particles S_1^E values of 0.00421 min^1.

Hence, more studies about the impact of the feed size distribution must be performed to try to understand the effect of the fine particles and at some point; it can be proposed a granulometry that has a low energy consumption and high production of fines (ideal size distribution). In this study, the variation in Mono size fraction, Coarse, Medium, and Fine size distributions is assumed as the starting point.

Nomenclature

a	Fracture speed, 1/min
B_s	Optimal ball size, mm
B_{ij}	Model ball mill breakage function
b_{ij}	Individual energy-based breakage function, showing the distribution of parent size class i to lower size j due to collision
D	inner mill diameter, m
F_{80}	Represents 80% passing size in the fresh feed stream
G(x)	Retained in "x" mesh, %
K_{100}	Passing 100% size in lineal function
M	Mass of the charge in the mill excluding the media
m	Slop in line equation
N	Mill speed, rpm
N_C	Mill critical speed expressed in percent
P	Is the basic mill power drawn
Q(x)	Correction factor for slow speed breakage
S_j	Breakage rate for size class j, 1/s
S_i^E	Energy-based breakage rate for size class I, t/kWh
S_i	Breakage rate for size class I, 1/s
S_1	Is the specific rate of breakage of size 1 and t is the grinding time

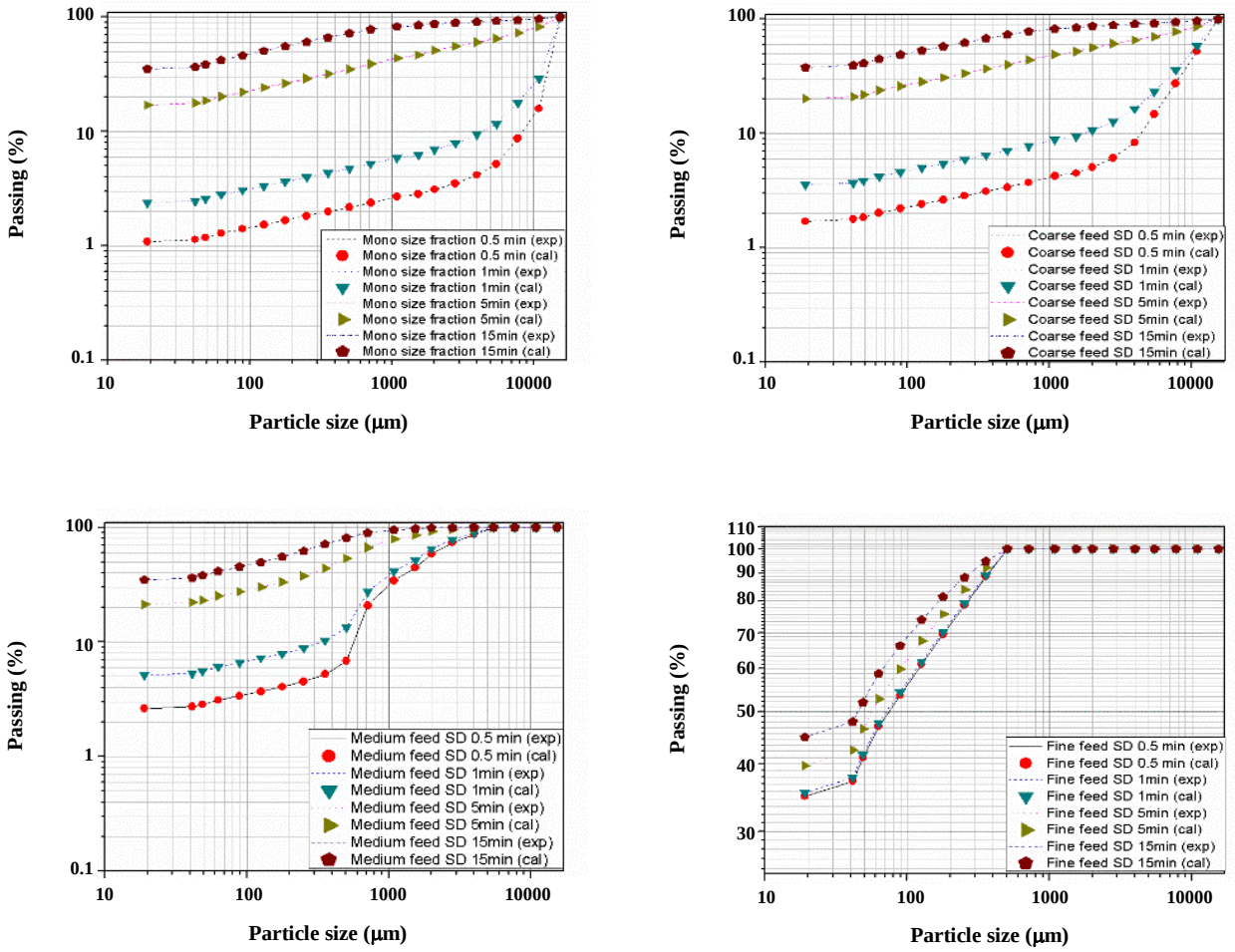

Fig. 9: Experimental and simulated cumulative passing data for mono size fraction, coarse, medium and fine feed size distributions.

T	Grinding time, min
w_i	Mass fraction for *i* class
W_{iB}	Bond´s work index, kWh/t
$W_1(t)$	The size fraction for particles size of class 1 at time t
$W_1(0)$	The size fraction for particles size of class 1 at time zero
X_i	The particle size, mm
X_0	Referent size, mm
α	Parameters dependent on the material ground
δ	Characterizes the degree of non-normalization
Λ	Index of how rapidly the rate of breakage falls away
μ	Factor that defines the particle size at which $Q(x)$ is 0.5
τ	Torque exerted by the mill minus friction in the bearings, Nm
∅	Parameter that depends on ore type

Acknowledgments

The authors thank to the Ministry of Education for financial support through the project of new PTC (project PRODEP).

Received : Aug. 16, 2019 ; Accepted :Feb. 17, 2020

REFERENCES

[1] Bourgeois FS., "Single-Particle Fracture as a Basis for Microscale Modeling of Comminution Process", Ph.D. Thesis. Department of Metallurgical Engineering, University of Utah (1993).

[2] Tavares L.M., Carvalho R.M., Modeling Breakage Rates of Coarse Particles in Ball Mills, *Miner. Eng.*, **22(7–8)**: 650–659 (2009).

[3] Tuzcu E.T., Rajamani R.K., Modeling Breakage Rates in Mills with Impact Energy Spectra and Ultra-Fast Load Cell Data, *Miner. Eng.*, **24(3–4)**: 252–260 (2011).

[4] Bhattacharyya A., Tuzcu E.T., Rajamani R., Experimental Study on Non-Linear Behavior of Breakage Rate Due to Fines Generation in Wet Batch Milling, *Miner. Eng.*, **99**: 19-29 (2016).

[5] Herbst J.A., Grandy G.A., Fuerstenau D.W., "Population Balance Models for the Design of Continuous Grinding Mills", *International Mineral Processing Congress*, April, London, (1973).

6] Austin L.G., Brame, K., A Comparison of Bond Method for Sizing Wet Tumbling Ball Mills with a Size-Mass Balance Simulation Model, *Powder Technol.*, **34(2)**: 261–274 (1983).

[7] Herbst J. A., Fuerstenau D.W., Mathematical Simulation of Dry Ball Milling Using Specific Power Information, *Trans. SME-AIME*, **254**: 343–348 (1973).

[8] Broadbent S.R., Callcott T.G., A Matrix Analysis of Processes Involving Particle Assembly, *Philos. Trans. R. Soc. London, Ser. A*, **249**: 99– 123 (1956)

[9] Nomura S., Hosoda K., Tanaka T., An Analysis of the Selection Function for Mills Using Balls as Grinding Media, *Powder Technol.*, **68**: 1–12 (1991).

[10] Datta A., Rajamani R.K., A Direct Approach of Modeling Batch Grinding in Ball Mills Using Population Balance Principles and Impact Energy Distribution, *Int. J. Miner. Process.*, **64(4)**: 181–200 (2002).

[11] Vogel L., Peukert W., Breakage Behaviour of Different Materials–Construction of a Mastercurve for the Breakage Probability, *Powder Technol.*, **129(1–3)**: 101–110 (2003).

[12] Peukert W., Material Properties in Fine Grinding, *Int. J. Miner. Process.*, **74S(10)**: S3–S17 (2004).

[13] Bwalya M.M., Moys M.H., Hinde A.L., The Use of Discrete Element Method and Fracture Mechanics to Improve Grinding Rate Prediction, *Miner. Eng.*, **14(6)**: 565–573 (2001).

[14] Austin L.G., Shoji K., Bell D., Rate Equations for Non-Linear Breakage in Mills Due to Materials Effects, *Powder Technol.*, **31(1)**: 127–133 (1982).

[15] Austin L.G., Luckie P.T., Estimation of Non-Normalized Breakage Distribution Parameters from Batch Grinding, *Powder Technol.*, **5(5)**: 267–277 (1972).

[16] Herbst J.A., Rajamani R.K., Developing a Simulator for Ball Mill Scale−up−a Case Study. In: "Design and Installation of Comminution Circuits", Mular A.L., Jergensen G.V. (Editors). AIME, New York, 325–345 (1982).

[17] Hogg R., Fuerstenau D.W., Transverse Mixing in Rotating Cylinders, *Powder Technol.*, **6(3)**: 139–48 (1972).

[18] Bond F.C., Crushing and Grinding Calculations. Part I, *Br. Chem. Eng.*, **6(6)**: 378–385 (1961).

[19] Bond F.C., Crushing and Grinding Calculations. Part II, *Br. Chem. Eng.*, **6(8)**: 543–548 (1961).

[20] Spottiswood D.J., Kelly E.G., The Breakage Function; What Is It Really?, *Miner.Eng.*, **3(5)**: 405–414 (1990).

[21] Bilgili E., Scarlett B., Population Balance of Non-Linear Effects in Milling Processes, *Powder Technol.*, **153**: 59–71 (2005).

[22] Yekeler M., "Breakage and Morphological Parameters Determined by Laboratory Tests. In: Particle Breakage", Salman A.D., Ghadiri M. Hounslow M.J. (Editors), Elsevier B.V., 438–485 (2007).

[23] Austin L.G., Trimarchi T., Weymont N.P., An Analysis of Some Cases of Non-first-Order Breakage Rates, *Powder Technol.*, **17(1)**: 109–113 (1977).

[24] Katubilwa F.M., Moys M.H., Effect of Ball Size Distribution on Milling Rate, *Miner. Eng.*, **22**: 1283–1288 (2009).